Stem Cell Reports
Article

ISSCR

OPEN ACCESS

# *Hif-1α* Deletion May Lead to Adverse Treatment Effect in a Mouse Model of MLL-AF9-Driven AML

Talia Velasco-Hernandez,[1,*] Shamit Soneji,[1] Isabel Hidalgo,[1] Eva Erlandsson,[1] Jörg Cammenga,[3,4] and David Bryder[1,2,*]

[1]Division of Molecular Hematology, Lund Stem Cell Center, Lund University, BMC B12, Sölvegatan 17, 22184 Lund, Sweden
[2]Sahlgrenska Cancer Center, Gothenburg University, 40530 Gothenburg, Sweden
[3]Department of Hematology, Linköping University Hospital, 58183 Linköping, Sweden
[4]Department of Clinical and Experimental Medicine, Linköping University, 58183 Linköping, Sweden
*Correspondence: tvelasco@carrerasresearch.org (T.V.-H.), david.bryder@med.lu.se (D.B.)
https://doi.org/10.1016/j.stemcr.2018.11.023

## SUMMARY

Relapse of acute myeloid leukemia (AML) remains a significant clinical challenge due to limited therapeutic options and poor prognosis. Leukemic stem cells (LSCs) are the cellular units responsible for relapse in AML, and strategies that target LSCs are thus critical. One proposed potential strategy to this end is to break the quiescent state of LSCs, thereby sensitizing LSCs to conventional cytostatics. The hypoxia-inducible factor (HIF) pathway is a main driver of cellular quiescence and a potential therapeutic target, with precedence from both solid cancers and leukemias. Here, we used a conditional knockout *Hif-1α* mouse model together with a standard chemotherapy regimen to evaluate LSC targeting in AML. Contrary to expectation, our studies revealed that *Hif-1α*-deleted-leukemias displayed a faster disease progression after chemotherapy. Our studies thereby challenge the general notion of cancer stem cell sensitization by inhibition of the HIF pathway, and warrant caution when applying HIF inhibition in combination with chemotherapy in AML.

## INTRODUCTION

Acute myeloid leukemia (AML) is a clonal disorder characterized by a rapid accumulation of differentiation-arrested myeloid blasts. Remission can be achieved in most patients by a combination of cytarabine (AraC) and anthracycline therapy. However, few treatment improvements have arisen over the past decades (Rowe and Tallman, 2010) and 40%–60% of patients still relapse (Burnett et al., 2011; Yanada et al., 2008), which is associated in general with limited treatment options (Dohner et al., 2010).

Relapse is attributed to a minor subpopulation of cells referred to as leukemic stem cells (LSCs). LSCs are resilient to cytotoxic effects of chemotherapy, via mechanisms that include resistance to apoptosis, increased capacities to efflux drugs, and relative quiescence (Thomas and Majeti, 2017). This quiescence in turn underlies resistance to compounds that target energy metabolism (Essers and Trumpp, 2010).

Cellular quiescence is typically related to activation of hypoxia-signaling pathway, driven by hypoxia-inducible factor (HIF) complex, which constitutes a family of 3 heterodimeric transcription factors HIF-1, HIF-2, and HIF-3 (Flamme et al., 1997; Makino et al., 2002; Semenza and Wang, 1992). The oxygen-dependent regulation of HIFs depends on stabilization of an associated α subunit. Hence, at oxygen levels above 5%, the α subunit is proteasomally degraded. In contrast, under hypoxic conditions the α subunit is stabilized, dimerizes with constitutively expressed β subunit, and promotes transcription of target genes regulating key cellular processes such as angiogenesis, proliferation, metabolism, and apoptosis (Semenza, 2003).

The most primitive hematopoietic stem cells (HSCs) reside in hypoxic niches in the bone marrow (BM) (Morrison and Scadden, 2014). Thereby, HSCs are kept dormant and free of genetic changes that mostly occur during DNA replication. However, while HIF-1α signaling was reported to critically regulate HSC maintenance (Takubo et al., 2010), other studies showed that depletion of HIF-1α/HIF-2α had no such effect (Guitart et al., 2013). The HIF pathway has also been proposed to play important roles in AML, a notion supported by the preferential localization of chemotherapy-resistant AML cells to the hypoxic endosteal niche in the BM (Ishikawa et al., 2007). Accordingly, several studies have shown that loss of HIF-1/2 leads to abrogation of LSCs (Rouault-Pierre et al., 2013; Wang et al., 2011; Zhang et al., 2012). Contrasting these results are studies demonstrating that loss of HIF-1/2 does not impact on mouse models of AML, or alternatively can give rise to an even more severe leukemic phenotype (Velasco-Hernandez et al., 2014; Vukovic et al., 2015). Nonetheless, targeting hypoxia and HIFs has been considered a key anticancer approach (Frolova et al., 2012; Rouault-Pierre et al., 2013; Wang et al., 2011).

Here, we investigated the possibility to sensitize LSCs from a mouse model of AML to a clinically relevant chemotherapy regimen by targeting the hypoxia pathway via *Hif-1α*. Contrary to expectation, our work suggests a more

 

aggressive disease outcome upon *Hif-1α* deletion, which challenges the general use of hypoxia targeting for therapeutic benefit in AML.

## RESULTS

### Deletion of *Hif-1α* Accelerates the Progression of Chemotherapy-Treated Leukemia

To study effects of *Hif-1α* on the sensitivity of LSCs to chemotherapy, we bred *Hif-1α*$^{fl}$ mice (Ryan et al., 2000) with Rosa26Cre-ER$^{T2}$ mice (Ventura et al., 2007), generating a model that allows for *Hif-1α* deletion upon tamoxifen treatment (Figure S1A). c-Kit$^+$ cells from *Hif-1α*$^{fl/fl}$;Rosa26Cre-ER$^{T2/+}$ mice were transduced with MLL-AF9-GFP retrovirus and transplanted into mice, which led to development of MLL-AF9-driven AML. Primary leukemias were next used to study AML progression in secondary hosts.

After comparing two different chemotherapy protocols (Figure S1B), we used the one described by Zuber et al. (2009), which resulted in severely decreased white blood cells, erythrocytes, and platelets, akin to what is observed in human patients. We then titrated the latency of the disease using different leukemic cell doses (Figure S1C) and chose a dose of $10^4$ cells, which ensured a sufficiently long latency for posterior procedures. Cells from individual MLL-AF9-leukemic mice were transplanted into new recipients and subjected to *Hif-1α* deletion 10 days after transplantation, and to a standard chemotherapeutic protocol at day 20. As a control, we included mice injected with both vehicles but receiving no leukemic cells (Figure 1A).

Three days after the last injection, we started to observe mortality in the PBS group (Figure S2A). We collected peripheral blood (PB), BM, spleen, and liver samples from half of the cohort and analyzed multiple disease parameters (Figures 1B–1F and S2). As expected, disease progressed more slowly in the chemotherapy-treated (CTX) mice (Figures 1B–1F). More intriguingly, we observed a faster disease evolution upon *Hif-1α* deletion. This was seen in both CTX and PBS groups (Figures 1C–1F). When we assessed phenotypically more primitive GFP$^+$ c-Kit$^+$ or GFP$^+$ Lin$^-$ c-Kit$^+$ cells, we observed a higher abundance in the *Hif-1α*-deleted (*Hif-1α*$^{-/-}$) than in the *Hif-1α*-intact (*Hif-1α*$^{+/+}$) group after chemotherapy (Figures 1G, 1H, and S2). While these populations were very infrequent in BM of PBS groups, with no clear differences between *Hif-1α*$^{-/-}$ and *Hif-1α*$^{+/+}$ cells, a higher number of such cells upon *Hif-1α* deletion were observed in the spleens of the same animals. Taken together, these results demonstrate an increment of potential LSCs (c-Kit$^+$) upon *Hif-1α*$^{-/-}$ deletion, which was particularly significant after chemotherapy.

### Deletion of *Hif-1α* Does Not Decrease the Frequency of LSCs after Chemotherapy Treatment

To evaluate the impact of chemotherapy and *Hif-1α* deletion on LSCs more directly, we performed limiting dilution analysis (LDA) (Figure 2A).

For an *in vitro* approach, we sorted 4, 8, or 12 GFP$^+$ leukemic BM cells from each group into individual wells. Proliferation was next evaluated in both normoxic (20% oxygen) and hypoxic (1% oxygen) conditions (Figures 2B and 2E). We obtained the highest LSC frequency from PBS-*Hif-1α*$^{-/-}$ cells (1/12.3 and 1/21.7 in hypoxia or normoxia, respectively, means from 3 independent experiments). Within CTX-treated cells, *Hif-1α*$^{-/-}$ samples contained a higher LSC frequency compared with *Hif-1α*$^{+/+}$ cells (1/26.8 versus 1/47.1 in hypoxia, and 1/40.4 versus 1/94.4 in normoxia, respectively, means from 3 independent experiments), although this failed to reach statistical significance.

We next assessed LSC frequencies *in vivo*, injecting 10, $10^2$, $10^3$, or $10^4$ GFP$^+$ BM cells from each group into new recipients (Figure 2C). While transplantation of $10^3$ and $10^4$ cells resulted in 100% mortality, lower doses of 10 and $10^2$ cells indicated an LSC frequency highest in the PBS-*Hif-1α*$^{-/-}$ group (1/18.8). Among CTX-treated samples, we observed a higher LSC frequency in the *Hif-1α*$^{-/-}$ group (1/34.5) than in the *Hif-1α*$^{+/+}$ group (1/56.1) (Figures 2D and 2E).

Estimation of total number of LSCs in the BM (Figure 2F) demonstrated that deletion of *Hif-1α* fails to reduce LSC frequencies/numbers after chemotherapy.

### *Hif-1α* Deletion Affects Transcriptional Expression of Replication, Transcription, and Translation-Related Genes

Our data indicated that *Hif-1α* deletion contributed to a more rapid disease progression (Figure 1). To tease out a potential mechanism, we therefore conducted single-cell RNA sequencing on leukemic cells from the 4 evaluated settings (*Hif-1α*$^{-/-}$/*Hif-1α*$^{+/+}$ ± chemotherapy) (Figure 3A). Aggregated data were subjected to dimensionality reduction using the t-distributed stochastic neighbor embedding (t-SNE) method (Figure 3B), revealing dramatically different transcriptional profiles of cells following chemotherapy, but less different according to *Hif-1α* status. This indicates either a modification of transcription upon chemotherapy or, more likely, a selective survival regardless of *Hif-1α* status.

By K-means clustering, we divided the entire dataset into 10 different clusters. We observed that clusters with functions related to more differentiated cells (e.g., immune system process, response to interleukin-1/tumor necrosis factor, innate immunity or response to virus/interferon) were predominant in PBS samples, while

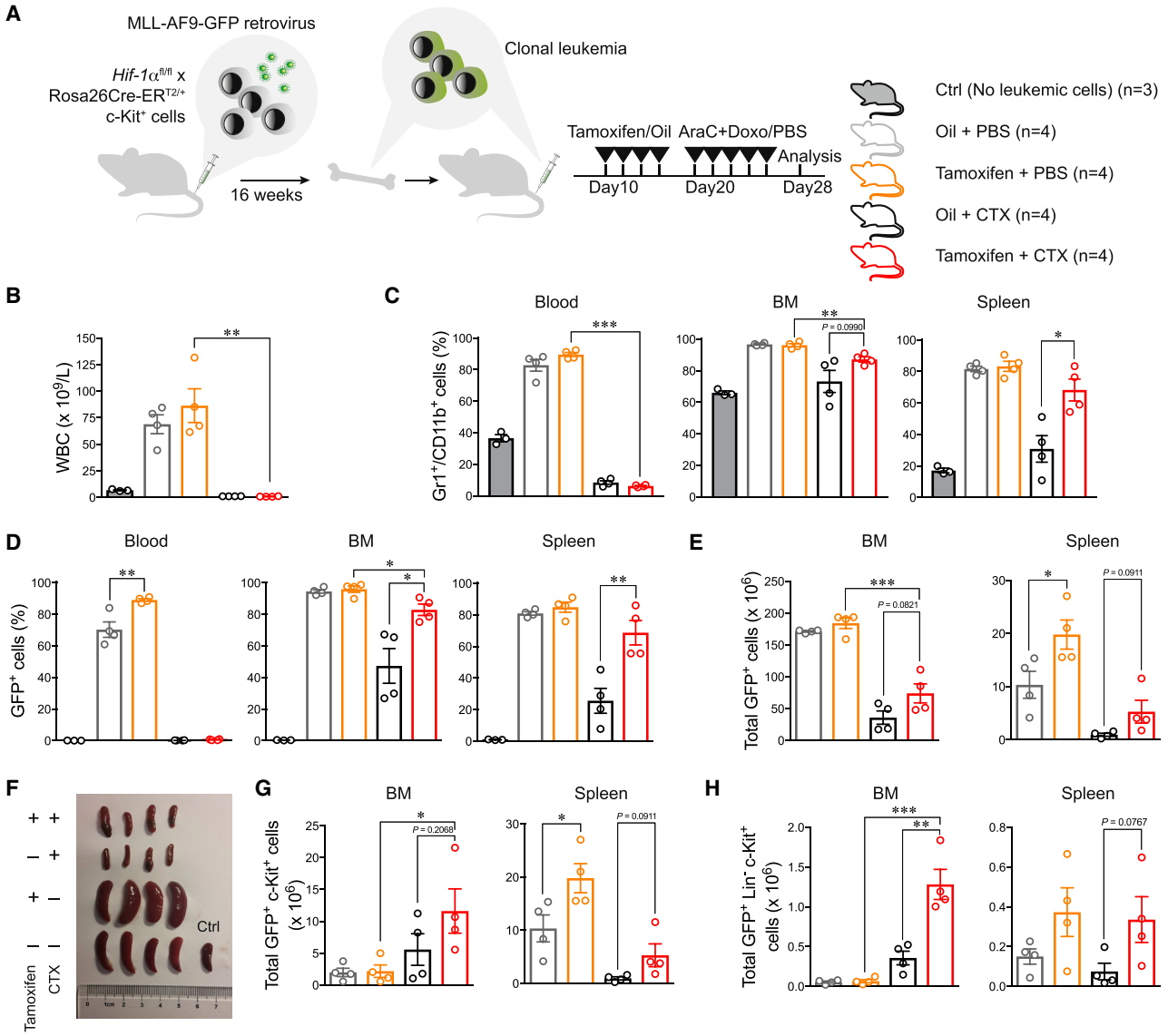


**Figure 1. Deletion of *Hif-1α* Leads to a Faster Progression of AML after Chemotherapy Treatment**

(A–H) Experimental design for the generation of leukemic clones, deletion of *Hif-1α*, and applied chemotherapy protocol (A). At day 28 after transplantation, mice were sacrificed and disease evolution was examined according to different parameters: total white blood cell count in PB (B), myeloid cells ($Gr1^+$-$CD11b^+$) (C), $GFP^+$ cells in PB, BM, and spleen (D and E), splenomegaly (F), $GFP^+$ c-$Kit^+$ cells in BM and spleen (G), and $GFP^+$ $Lin^-$ c-$Kit^+$ in BM and spleen (H). Results are from 1 of 2 experiments and depict results from 4 mice per group (3 for wild-type control mice). Plots represent mean ± SEM. *p < 0.05, **p < 0.01, ***p < 0.01. AraC, cytarabine; Dox, doxorubicin; CTX, chemotherapy; BM, bone marrow; Ctrl, control.

See also Figures S1 and S2.

others (e.g., mitotic cell cycle, cellular response to DNA damage, and transcriptional regulation) were associated with CTX samples. Multiple genes related to myeloid differentiation were predominantly expressed in PBS samples (data not shown), strongly suggesting effective chemotherapy targeting of more mature leukemia-associated cells.

Pairwise sample comparisons produced a collection of 331 differentially expressed genes (Figures S3 and 3C). When comparing significantly overexpressed genes among groups (adjusted p value <0.05), we found a very different distribution of cells between CTX and PBS samples, but only a small subset of genes uniquely expressed in either *Hif-1α*$^{-/-}$ or *Hif-1α*$^{+/+}$ cells (Figures 3D and S4). In

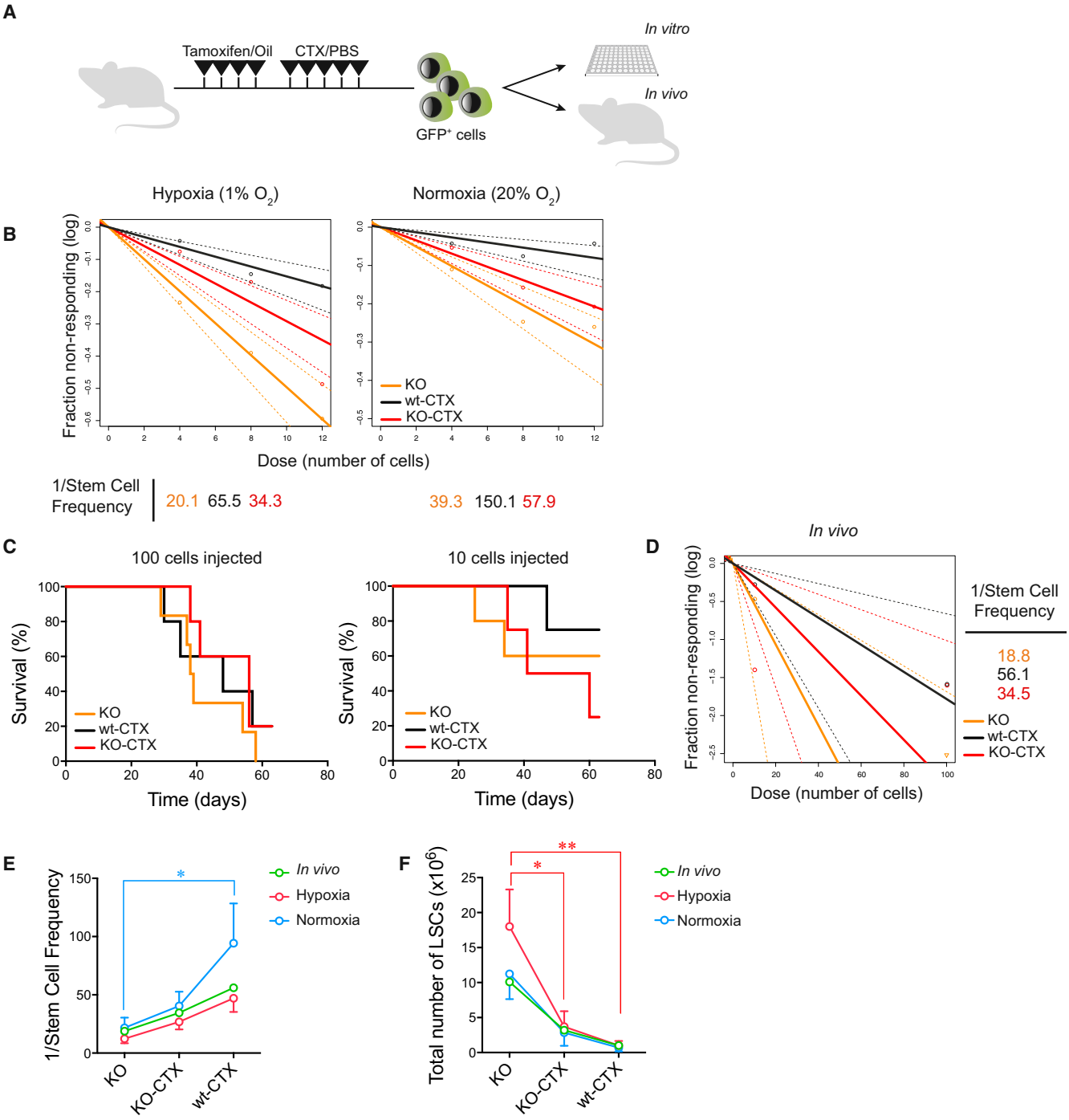


**Figure 2. Deletion of *Hif-1α* Does Not Decrease LSC Frequency after Chemotherapy**

(A) Experimental design for the analysis of LSC frequency.

(B) Limiting dilution analysis (LDA) from *in vitro* data. Variable numbers of GFP$^+$ cells (4, 8, or 12 cells) from the 3 experimental groups were cultured *in vitro* under normoxic or hypoxic conditions and proliferative capacity was evaluated after 10 days. LSC frequencies were calculated using ELDA software. Plots show 1 representative of 3 independent experiments (cells from 3 different donors) with 96 replicates per group and condition.

(C) Survival curves of mice transplanted with 10 or 100 GFP$^+$ cells from mice treated with the combination of tamoxifen + chemotherapy (KO-CTX), tamoxifen + PBS (KO-PBS), or oil + chemotherapy (wt-CTX) (n = 4–6 mice per group from 1 experiment).

*(legend continued on next page)*

single-cell analysis, this indicates that there are differences in transcriptional regulation or that analyzed cells from each sample are different.

To identify functional protein association networks among differentially expressed genes, we used the STRING database (Figures 3E and 4). For the 4 sets of differentially expressed genes (log fold change >0.4, adjusted p value <0.05), we obtained a significant protein-protein interaction (PPI) enrichment score, indicating that there are more interactions among these proteins than a random set of proteins from the genome (PPI enrichment p values: *Hif-1α*$^{-/-}$-CTX = 0; *Hif-1α*$^{+/+}$-CTX = $1.03 \times 10^{-6}$; *Hif-1α*$^{-/-}$-PBS = 0; *Hif-1α*$^{+/+}$-PBS = 0.0251). This indicates that genes in each set are at least partially biologically connected. To correlate these genes with a biological function, we performed gene ontology and KEGG pathway enrichment analyses (Figure 3E). This revealed that mRNA processing, DNA replication, and protein folding were significantly overrepresented in the *Hif-1α*$^{-/-}$-CTX group, while the *Hif-1α*$^{+/+}$-CTX group was associated with the HIF-1α pathway, glycolysis, and other carbon metabolism processes. In PBS groups, translation was the most represented pathway associated with *Hif-1α*$^{-/-}$ cells, while no significant pathways could be assigned to *Hif-1α*$^{+/+}$ cells.

## DISCUSSION

Relapse of AML remains a major therapeutic challenge, not least because of the few therapeutic options for many of these patients, which in most cases is restricted to palliative care.

One potential strategy for eradicating LSCs, responsible for relapse in AML, is to sensitize them to chemotherapy. We here explored whether targeting the HIF pathway could be used for this using an MLL-AF9 murine AML model, which was subjected to a standard and clinically relevant chemotherapy protocol. In our work, *Hif-1α*$^{-/-}$ cells displayed a faster evolution of the disease compared with *Hif-1α*$^{+/+}$ cells following chemotherapy. While the results are consistent with our previous work (Velasco-Hernandez et al., 2014) and recently published data (Vukovic et al., 2015), they appear in sharp contrast to previous studies (Wang et al., 2011; Zhang et al., 2012) in which *Hif-1α* was critical for LSCs maintenance.

In our work, we used the Rosa26Cre-ER$^{T2}$ rather than the more commonly used Mx1-Cre model, which is associated with significant leakiness (Velasco-Hernandez et al., 2016). This allowed us to study the effect of *Hif-1α* inhibition specifically in AML cells of the same founder clone, which circumvents the risk that different leukemic clones have intrinsically different behavior. Inducing the deletion in Rosa26Cre-ER$^{T2}$ mice requires injection of tamoxifen that might itself affect the initiation of MLL-AF9 leukemia (Sanchez-Aguilera et al., 2014). However, as the described effect of tamoxifen is a regression of the disease, the isolated effect of knocking out *Hif-1α* could be even more pronounced than the one we report.

The standard chemotherapy regimen for AML is a combination of AraC and an anthracycline (such as doxorubicin). Doxorubicin has itself been attributed *Hif*-inhibiting properties (Lee et al., 2009). Different disease progression in CTX-*Hif-1α*$^{-/-}$ and *Hif-1α*$^{+/+}$ samples indicates that even if doxorubicin is inhibiting HIF function, this effect is not complete and can be further increased by alternative means.

There is evidence that c-Kit deregulation and overexpression could be factors contributing to the chemotherapy resistance in AML (Advani et al., 2008). The higher numbers of c-Kit$^{+}$ cells in the *Hif-1α*$^{-/-}$ chemotherapy group might therefore be an indicator of higher drug resistance of these cells, with c-Kit being a well-described stem cell marker of murine MLL-AF9-driven LSCs (Krivtsov et al., 2006). However, our c-Kit expression data correlated poorly with LSC frequencies measured by LDA. Previously it was thought that chemotherapy promoted LSC enrichment (Ishikawa et al., 2007; Saito et al., 2010). However, although cytarabine decreases the frequency of LSCs in human AML models (Griessinger et al., 2014), it fails to promote enrichment either of quiescent cells or more primitive CD34$^{+}$CD38$^{-}$ cells, emphasizing that functional assessments are critical. We did not observe an increment in LSC frequencies measured by LDA but observed a substantial reduction (around 3-fold) of the total bulk of leukemic cells, indicating an overall enrichment of LSCs following chemotherapy. In addition, we observed an increased frequency of c-Kit$^{+}$ cells by *Hif-1α* deletion, which further supports the increased aggressive phenotype of *Hif-1α*$^{-/-}$ cells.

*Hif-1α* is rapidly degraded in normoxia and *Hif-1α*$^{+/+}$ cells should thus theoretically behave as *Hif-1α*$^{-/-}$ cells, which

(D) LDA from *in vivo* data. Recipient mice were injected intravenously with variable numbers of GFP$^{+}$ cells from the 3 experimental groups (KO-CTX, KO-PBS, and wt-CTX). Mice survival was evaluated 2 months after transplantation, and frequency of LSCs was calculated using ELDA software.

(E) Stem cell frequency of LSCs from the different experiments: hypoxia *in vitro* (red, n = 3), normoxia *in vitro* (blue, n = 3), and *in vivo* (green, n = 1) experiments. *p < 0.05, two-way ANOVA.

(F) LSC total numbers from the different experiments: hypoxia *in vitro* (red, n = 3), normoxia *in vitro* (blue, n = 3), and *in vivo* (green, n = 1) experiments. Plot shows mean ± SEM. *p < 0.05, **p < 0.01, two-way ANOVA. CTX, chemotherapy; KO, *Hif-1α*$^{-/-}$; wt, *Hif-1α*$^{+/+}$.

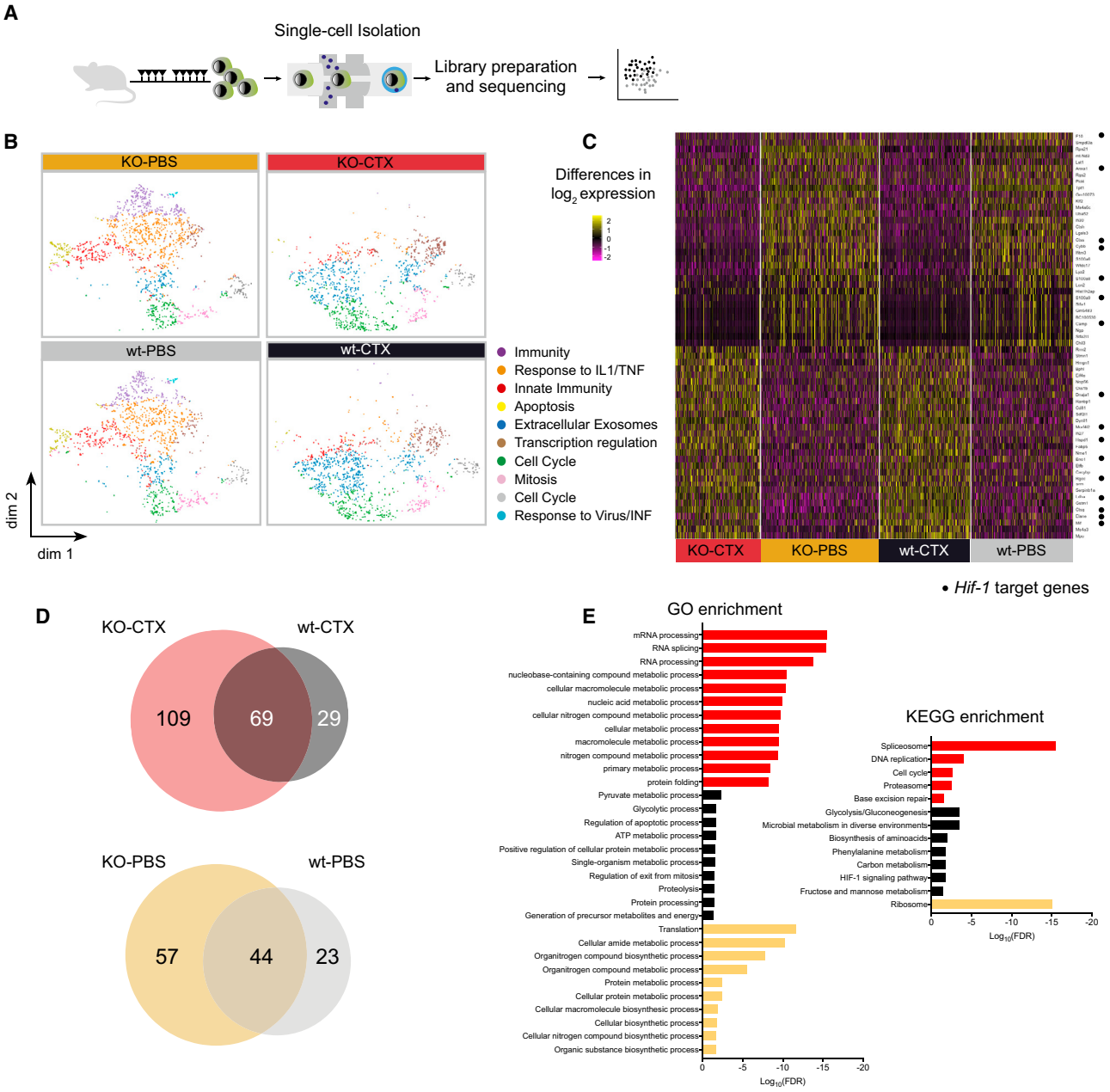


**Figure 3. Single-Cell RNA Sequencing of Leukemic Cells after Chemotherapy Treatment**

(A) Experimental design for single-cell RNA-sequencing analysis. After treatment with tamoxifen/oil and chemotherapy/PBS, $GFP^+$ cells were collected at day 28 after transplantation and subjected to RNA processing.

(B) t-SNE plots representing gene expression profiles of all individual cells analyzed: KO-CTX (n = 1,217 cells), KO-PBS (n = 1,696 cells), wt-CTX (n = 1,301 cells), and wt-PBS (n = 1,450 cells). Each dot represents one cell. K-means clustering groups cells into 10 clusters, which are represented by different colors. Differentially expressed genes in each cluster were correlated with the main biological function indicated at the right side of the plots.

(C) Heatmap depicting significantly differentially expressed genes in single cells. Heatmap with the full set of genes can be found in Figure S3. *Hif-1α* target genes are indicated by black dots.

(D) Venn diagrams showing the distribution among groups of differentially expressed genes (adjusted p value <0.05). Of note, there are no overlapping genes between chemotherapy- and PBS-treated groups among this set of differentially expressed genes.

*(legend continued on next page)*

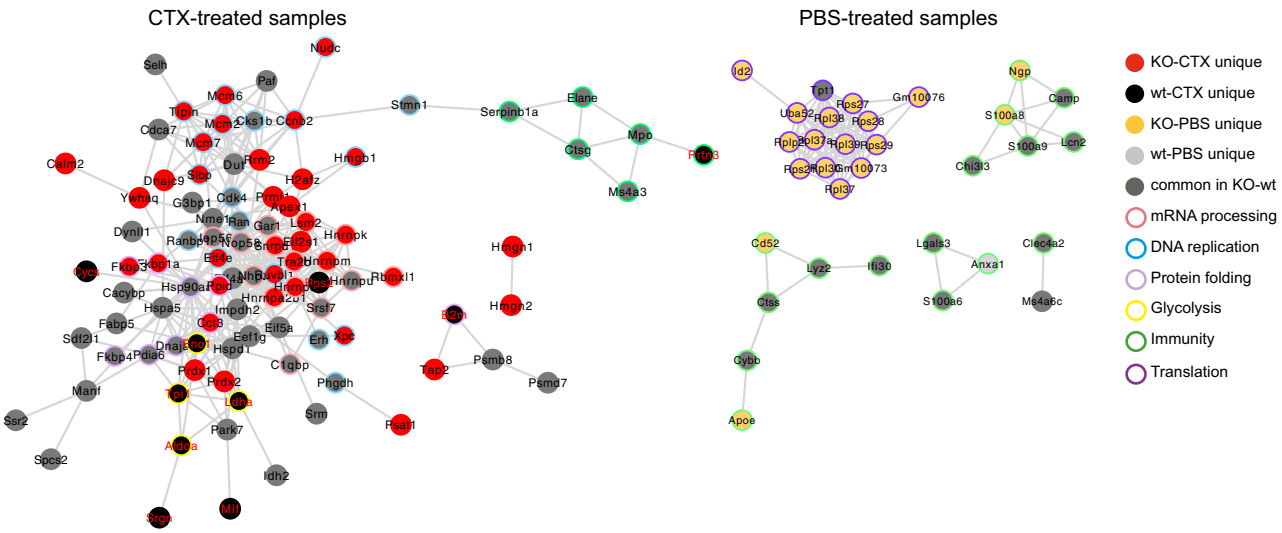


| CTX-treated Samples | | | | | | PBS-treated Samples | | |
|---|---|---|---|---|---|---|---|---|
| KO unique | | wt unique | KO-wt common | | | KO unique | wt unique | KO-wt common |
| Apex1 | Mcm6 | Aldoa | C1qbp | Hnrnpu | Ran | Apoe | Anxa1 | Camp |
| Calm2 | Mcm7 | B2m | Cacybp | Hsp90aa | Ranbp1 | Cd52 | | Chi3l3 |
| Ccnb2 | Nudc | Cycs | Cdca7 | Hspa5 | Sdf2l1 | Gm10073 | | Clec4a2 |
| Cct3 | Ppid | Eno1 | Cdk4 | Hspd1 | Selh | Gm10076 | | Ctss |
| Dnajc9 | Prdx1 | Ldha | Cks1b | Idh2 | Serpinb1a | Id2 | | Cybb |
| Eif2s1 | Prdx2 | Mif | Ctsg | Impdh2 | Spcs2 | Ngp | | Ifi30 |
| Eif4e | Prmt1 | Prtn3 | Dnaja1 | Manf | Srm | Rpl30 | | Lcn2 |
| Fkbp1a | Psat1 | Rps2 | Dut | Mpo | Srsf7 | Rpl37 | | Lgals3 |
| Fkbp3 | Rbmxl1 | Srgn | Dynll1 | Ms4a3 | Ssr2 | Rpl37a | | Lyz2 |
| H2afz | Rrm2 | Tpi1 | Eef1g | Nhp2 | Stmn1 | Rpl38 | | Ms4a6c |
| Hmgb1 | Ruvbl1 | | Eif4a1 | Nme1 | | Rpl39 | | S100a6 |
| Hmgn1 | Slbp | | Eif5a | Nop56 | | Rplp2 | | S100a9 |
| Hmgn2 | Snrpd | | Elane | Nop58 | | Rps21 | | Tpt1 |
| Hnrnpa2b1 | Tap2 | | Erh | Paf | | Rps28 | | |
| Hnrnpc | Tipin | | Fabp5 | Park7 | | Rps29 | | |
| Hnrnpk | Tra2b | | Fabp5 | Pdia6 | | Rsp27 | | |
| Hnrnpm | Xpc | | Fkbp4 | Phgdh | | S100a8 | | |
| Lsm2 | Ywhaq | | G3bp1 | Psmb8 | | Uba52 | | |
| Mcm2 | | | Gar1 | Psmd7 | | | | |

**Figure 4. Protein Association Networks Affected by Chemotherapy**

Protein association network analysis of differentially expressed set of genes (average log fold change >0.4, adjusted p value <0.05). Uniquely expressed genes from each group are indicated by its assigned color. Common genes among KO and wt samples, within each specific set (CTX- or PBS-treated), are shown in dark gray. Associated biological function to each gene is indicated, with the color of the border showing the main processes regulated by these genes. Interaction enrichment score >0.5. CTX, chemotherapy.

would suggest similar LSC frequencies between *Hif-1α*$^{-/-}$ and *Hif-1α*$^{+/+}$ cells in normoxia. Somewhat surprisingly, we observed a higher LSC frequency of *Hif-1α*$^{-/-}$ cells, although not significant (p = 0.1079). One possibility is that this indicates the involvement of one or more *Hif-1α*-oxygen-independent mechanisms. For instance, it is well established that *Hif-1α* can be induced by the PTEN/PI3K/AKT axis (Zundel et al., 2000), a pathway that appears to extend also to MLL-AF9 leukemia (Hoshii et al., 2012). Regardless, even if hypoxia in general promotes a quiescent state of cells, such conditions seem to promote AML cell proliferation, which is also in line with previous results on human AML (Griessinger et al., 2014).

After chemotherapy, we observed a more aggressive phenotype as a consequence of *Hif-1α* deletion. We hypothesized that this faster development of disease could

(E) Gene ontology (GO) and KEGG pathway enrichment analysis from uniquely differentially expressed genes in each group indicating the associated biological process.

CTX, chemotherapy; IL1/TNF, interleukin-1/tumor necrosis factor; INF, interferon; dim, dimension; FDR, false discovery rate.

See also Figures S3 and S4.

be explained by two scenarios: (1) leukemic *Hif-1α*$^{-/-}$ cells are less sensitive to the chemotherapy, which would be in contrast to our original expectation; and/or (2) leukemic *Hif-1α*$^{-/-}$ cells expand faster than *Hif-1α*$^{+/+}$ cells after chemotherapy. To discriminate between these two options and unveil possible mechanisms leading to this effect, we conducted a single-cell transcriptome analysis.

We found that chemotherapy-treated cells displayed a distinct transcriptomic profile when compared with PBS-treated cells, but with fewer differences when comparing *Hif-1α*$^{-/-}$ and *Hif-1α*$^{+/+}$ cells. Still, of the significantly over-expressed genes specific for each group, we identified an increment in genes involved in translation (PBS-*Hif-1α*$^{-/-}$ cells) and in mRNA processing, DNA replication, and protein folding (CTX-*Hif-1α*$^{-/-}$ cells). Overall, this is in line with a more active proliferative status of *Hif-1α*$^{-/-}$ cells and suggests that deletion of *Hif-1α* is transcriptionally deregulating these aforementioned specific pathways. Chemotherapy-depleted cells with an immune-related phenotype represent the cells expanded in leukemia. As expected, *Hif-1α*$^{-/-}$ cells were depleted in expression of *Hif-1α* targets, and *Hif-1α* deletion leads to an enhanced transcription of genes involved mainly in replication, mRNA processing, and translation.

These results are in accordance with the described effect of *Hif-1α*, inhibiting cell cycle and promoting quiescence, actions attributed to blockage of c-MYC and enhancement of cyclin-dependent kinase inhibitors such as p21/CDKN1A (Koshiji et al., 2004). Since we are deleting only one member of a multigene family, it remains a possibility that other members, i.e., *Hif-2α*, could have a compensatory effect. Future work could benefit from an increased understanding of both gene redundancy and potential hypoxia-independent effects of *Hif-1α*.

Overall, our data suggest that *Hif-1α* inhibition failed to improve the outcome of chemotherapy in MLL-AF9-driven AML and, in contrast, led to a faster progression of disease upon withdrawal of the treatment. Further investigations are needed to extend these conclusions to other genetic subtypes of AML.

Deletion of *Hif-1α* in our setting was permanent, which would be a different scenario than in a clinical setting where administration of *Hif-1α* inhibitors would be transient. Our results nevertheless emphasize that the effects of HIF inhibition have to be further investigated before this strategy can be applied in a clinical setting.

## EXPERIMENTAL PROCEDURES

### Mice

*Hif-1α*$^{lox}$ mice (Ryan et al., 2000) (JAX 007561) were crossed with the tamoxifen-inducible Rosa26Cre-ER$^{T2}$ mice (Ventura et al., 2007) (JAX 008463) to generate a combined conditional knockout (KO) model. Mice were maintained at the animal facility of the Biomedical Center at Lund University (Sweden) and all experiments were performed with consent from a local ethics committee.

### Statistical Analysis

All data are expressed as the mean ± SEM. Differences between groups were assessed using unpaired Student's t tests. All analyses were performed with Prism software, version 7.0 (GraphPad Software).

Detailed descriptions of experiments can be found in Supplemental Experimental Procedures.

## ACCESSION NUMBERS

The accession number for transcriptomic data is GEO: GSE119484.

## SUPPLEMENTAL INFORMATION

Supplemental Information includes Supplemental Experimental Procedures and four figures and can be found with this article online at https://doi.org/10.1016/j.stemcr.2018.11.023.

## AUTHOR CONTRIBUTIONS

T.V.-H. designed the study, performed experiments, analyzed data, and wrote the manuscript; S.S. performed bioinformatics analysis; I.H. and E.E. performed experiments; and J.C and D.B. designed the study and wrote the manuscript. All authors revised the manuscript and approved the final version of this study.

## ACKNOWLEDGMENTS

We thank Dr. Göran Karlsson and Parashar Dhapola for helpful discussions on data analysis. This work was supported with a project grant to T.V.-H. from the Sigurd och Elsa Goljes Minne Memorial Foundation, to J.C. from The Swedish Cancer Society (Cancerfonden) and Barncancerfonden, and to D.B. from The Swedish Cancer Society, The Swedish Medical Research Council, ERC (Leukemiabarrier 615068), The Knut and Alice Wallenberg Foundation, and the Tobias Foundation.

Received: September 11, 2018
Revised: November 30, 2018
Accepted: November 30, 2018
Published: December 27, 2018

## REFERENCES

Advani, A.S., Rodriguez, C., Jin, T., Jawde, R.A., Saber, W., Baz, R., Kalaycio, M., Sobecks, R., Sekeres, M., Tripp, B., et al. (2008). Increased C-kit intensity is a poor prognostic factor for progression-free and overall survival in patients with newly diagnosed AML. Leuk. Res. *32*, 913–918.

Burnett, A., Wetzler, M., and Lowenberg, B. (2011). Therapeutic advances in acute myeloid leukemia. J. Clin. Oncol. *29*, 487–494.

Dohner, H., Estey, E.H., Amadori, S., Appelbaum, F.R., Buchner, T., Burnett, A.K., Dombret, H., Fenaux, P., Grimwade, D., Larson, R.A., et al. (2010). Diagnosis and management of acute myeloid leukemia in adults: recommendations from an international expert

panel, on behalf of the European Leukemianet. Blood *115*, 453–474.

Essers, M.A., and Trumpp, A. (2010). Targeting leukemic stem cells by breaking their dormancy. Mol. Oncol. *4*, 443–450.

Flamme, I., Frohlich, T., von Reutern, M., Kappel, A., Damert, A., and Risau, W. (1997). HRF, a putative basic helix-loop-helix-PAS-domain transcription factor is closely related to hypoxia-inducible factor-1 alpha and developmentally expressed in blood vessels. Mech. Dev. *63*, 51–60.

Frolova, O., Samudio, I., Benito, J.M., Jacamo, R., Kornblau, S.M., Markovic, A., Schober, W., Lu, H., Qiu, Y.H., Buglio, D., et al. (2012). Regulation of HIF-1alpha signaling and chemoresistance in acute lymphocytic leukemia under hypoxic conditions of the bone marrow microenvironment. Cancer Biol. Ther. *13*, 858–870.

Griessinger, E., Anjos-Afonso, F., Pizzitola, I., Rouault-Pierre, K., Vargaftig, J., Taussig, D., Gribben, J., Lassailly, F., and Bonnet, D. (2014). A niche-like culture system allowing the maintenance of primary human acute myeloid leukemia-initiating cells: a new tool to decipher their chemoresistance and self-renewal mechanisms. Stem Cells Transl. Med. *3*, 520–529.

Guitart, A.V., Subramani, C., Armesilla-Diaz, A., Smith, G., Sepulveda, C., Gezer, D., Vukovic, M., Dunn, K., Pollard, P., Holyoake, T.L., et al. (2013). Hif-2alpha is not essential for cell-autonomous hematopoietic stem cell maintenance. Blood *122*, 1741–1745.

Hoshii, T., Tadokoro, Y., Naka, K., Ooshio, T., Muraguchi, T., Sugiyama, N., Soga, T., Araki, K., Yamamura, K., and Hirao, A. (2012). mTORC1 is essential for leukemia propagation but not stem cell self-renewal. J. Clin. Invest. *122*, 2114–2129.

Ishikawa, F., Yoshida, S., Saito, Y., Hijikata, A., Kitamura, H., Tanaka, S., Nakamura, R., Tanaka, T., Tomiyama, H., Saito, N., et al. (2007). Chemotherapy-resistant human AML stem cells home to and engraft within the bone-marrow endosteal region. Nat. Biotechnol. *25*, 1315–1321.

Koshiji, M., Kageyama, Y., Pete, E.A., Horikawa, I., Barrett, J.C., and Huang, L.E. (2004). HIF-1alpha induces cell cycle arrest by functionally counteracting Myc. EMBO J. *23*, 1949–1956.

Krivtsov, A.V., Twomey, D., Feng, Z., Stubbs, M.C., Wang, Y., Faber, J., Levine, J.E., Wang, J., Hahn, W.C., Gilliland, D.G., et al. (2006). Transformation from committed progenitor to leukaemia stem cell initiated by MLL-AF9. Nature *442*, 818–822.

Lee, K., Qian, D.Z., Rey, S., Wei, H., Liu, J.O., and Semenza, G.L. (2009). Anthracycline chemotherapy inhibits HIF-1 transcriptional activity and tumor-induced mobilization of circulating angiogenic cells. Proc. Natl. Acad. Sci. U S A *106*, 2353–2358.

Makino, Y., Kanopka, A., Wilson, W.J., Tanaka, H., and Poellinger, L. (2002). Inhibitory PAS domain protein (IPAS) is a hypoxia-inducible splicing variant of the hypoxia-inducible factor-3alpha locus. J. Biol. Chem. *277*, 32405–32408.

Morrison, S.J., and Scadden, D.T. (2014). The bone marrow niche for haematopoietic stem cells. Nature *505*, 327–334.

Rouault-Pierre, K., Lopez-Onieva, L., Foster, K., Anjos-Afonso, F., Lamrissi-Garcia, I., Serrano-Sanchez, M., Mitter, R., Ivanovic, Z., de Verneuil, H., Gribben, J., et al. (2013). HIF-2alpha protects human hematopoietic stem/progenitors and acute myeloid leukemic cells from apoptosis induced by endoplasmic reticulum stress. Cell Stem Cell *13*, 549–563.

Rowe, J.M., and Tallman, M.S. (2010). How I treat acute myeloid leukemia. Blood *116*, 3147–3156.

Ryan, H.E., Poloni, M., McNulty, W., Elson, D., Gassmann, M., Arbeit, J.M., and Johnson, R.S. (2000). Hypoxia-inducible factor-1alpha is a positive factor in solid tumor growth. Cancer Res. *60*, 4010–4015.

Saito, Y., Uchida, N., Tanaka, S., Suzuki, N., Tomizawa-Murasawa, M., Sone, A., Najima, Y., Takagi, S., Aoki, Y., Wake, A., et al. (2010). Induction of cell cycle entry eliminates human leukemia stem cells in a mouse model of AML. Nat. Biotechnol. *28*, 275–280.

Sanchez-Aguilera, A., Arranz, L., Martin-Perez, D., Garcia-Garcia, A., Stavropoulou, V., Kubovcakova, L., Isern, J., Martin-Salamanca, S., Langa, X., Skoda, R.C., et al. (2014). Estrogen signaling selectively induces apoptosis of hematopoietic progenitors and myeloid neoplasms without harming steady-state hematopoiesis. Cell Stem Cell *15*, 791–804.

Semenza, G.L. (2003). Targeting HIF-1 for cancer therapy. Nat. Rev. Cancer *3*, 721–732.

Semenza, G.L., and Wang, G.L. (1992). A nuclear factor induced by hypoxia via de novo protein synthesis binds to the human erythropoietin gene enhancer at a site required for transcriptional activation. Mol. Cell. Biol. *12*, 5447–5454.

Takubo, K., Goda, N., Yamada, W., Iriuchishima, H., Ikeda, E., Kubota, Y., Shima, H., Johnson, R.S., Hirao, A., Suematsu, M., et al. (2010). Regulation of the HIF-1alpha level is essential for hematopoietic stem cells. Cell Stem Cell *7*, 391–402.

Thomas, D., and Majeti, R. (2017). Biology and relevance of human acute myeloid leukemia stem cells. Blood *129*, 1577–1585.

Velasco-Hernandez, T., Hyrenius-Wittsten, A., Rehn, M., Bryder, D., and Cammenga, J. (2014). HIF-1alpha can act as a tumor suppressor gene in murine acute myeloid leukemia. Blood *124*, 3597–3607.

Velasco-Hernandez, T., Sawen, P., Bryder, D., and Cammenga, J. (2016). Potential pitfalls of the Mx1-Cre system: implications for experimental modeling of normal and malignant hematopoiesis. Stem Cell Reports *7*, 11–18.

Ventura, A., Kirsch, D.G., McLaughlin, M.E., Tuveson, D.A., Grimm, J., Lintault, L., Newman, J., Reczek, E.E., Weissleder, R., and Jacks, T. (2007). Restoration of p53 function leads to tumour regression in vivo. Nature *445*, 661–665.

Vukovic, M., Guitart, A.V., Sepulveda, C., Villacreces, A., O'Duibhir, E., Panagopoulou, T.I., Ivens, A., Menendez-Gonzalez, J., Iglesias, J.M., Allen, L., et al. (2015). Hif-1alpha and Hif-2alpha synergize to suppress AML development but are dispensable for disease maintenance. J. Exp. Med. *212*, 2223–2234.

Wang, Y., Liu, Y., Malek, S.N., Zheng, P., and Yang, L. (2011). Targeting HIF1alpha eliminates cancer stem cells in hematological malignancies. Cell Stem Cell *8*, 399–411.

Yanada, M., Garcia-Manero, G., Borthakur, G., Ravandi, F., Kantarjian, H., and Estey, E. (2008). Relapse and death during first remission in acute myeloid leukemia. Haematologica *93*, 633–634.

Zhang, H., Li, H., Xi, H.S., and Li, S. (2012). HIF1alpha is required for survival maintenance of chronic myeloid leukemia stem cells. Blood *119*, 2595–2607.

Zuber, J., Radtke, I., Pardee, T.S., Zhao, Z., Rappaport, A.R., Luo, W., McCurrach, M.E., Yang, M.M., Dolan, M.E., Kogan, S.C., et al. (2009). Mouse models of human AML accurately predict chemotherapy response. Genes Dev. *23*, 877–889.

Zundel, W., Schindler, C., Haas-Kogan, D., Koong, A., Kaper, F., Chen, E., Gottschalk, A.R., Ryan, H.E., Johnson, R.S., Jefferson, A.B., et al. (2000). Loss of PTEN facilitates HIF-1-mediated gene expression. Genes Dev. *14*, 391–396.

**Stem Cell Reports, Volume *12***

## Supplemental Information

# *Hif-1α* Deletion May Lead to Adverse Treatment Effect in a Mouse Model of MLL-AF9-Driven AML

**Talia Velasco-Hernandez, Shamit Soneji, Isabel Hidalgo, Eva Erlandsson, Jörg Cammenga, and David Bryder**

## Supplemental Information

# *Hif-1α* deletion may lead to adverse treatment effect in a mouse model of MLL-AF9 driven AML

**Authors:**

Talia Velasco-Hernandez[1*], Shamit Soneji[1], Isabel Hidalgo[1], Eva Erlandsson[1], Jörg Cammenga[2,3] and David Bryder[1*]

Supplemental Figure S1. Velasco-Hernandez et al

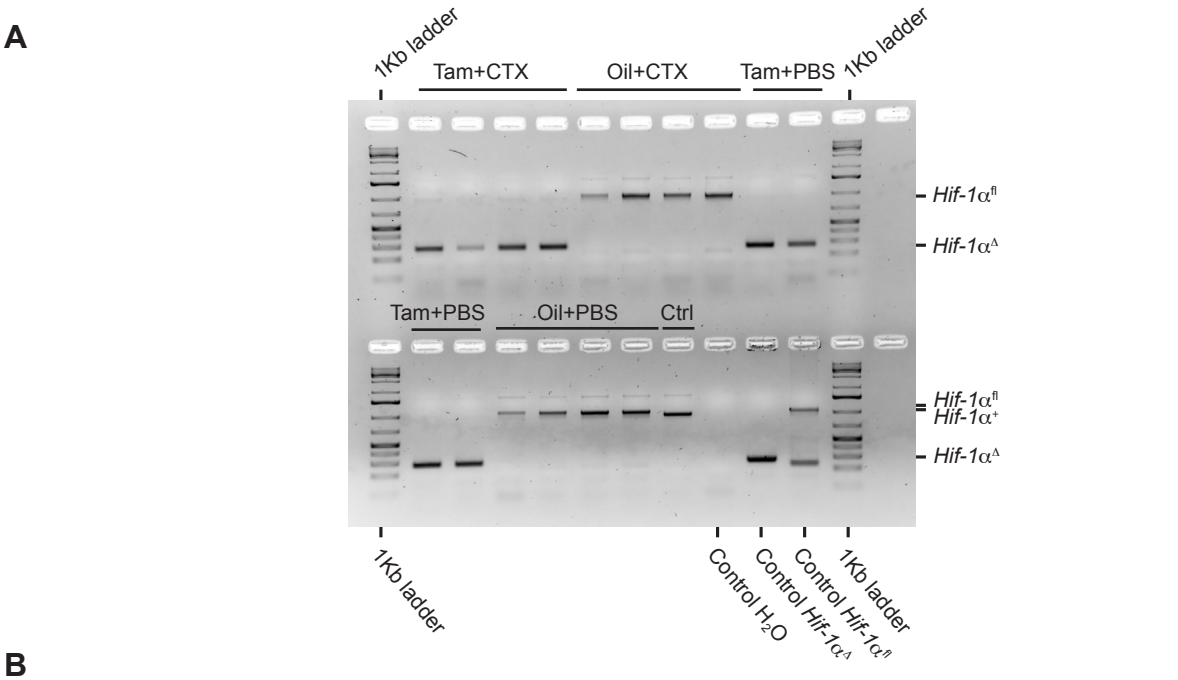


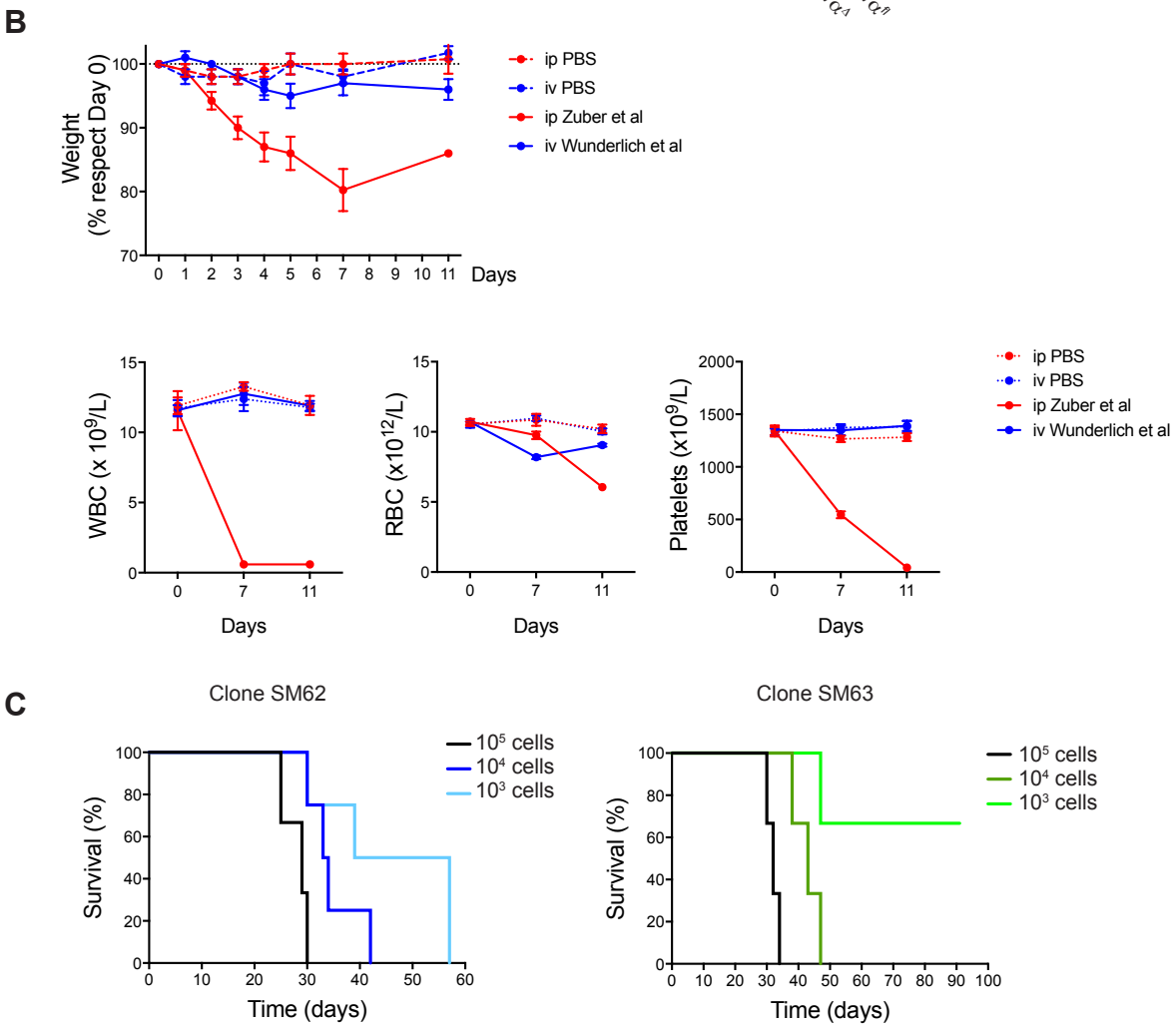

**Supplemental Figure 1, related to Figure 1.**

**A.** PCR analysis to check deletion of *Hif-1α* gene after treatment with tamoxifen. Genomic DNA was extracted from BM cells at day 28 after transplantation and PCR was performed to check deletion of *Hif-1α*. Only in samples from mice treated with tamoxifen we can observe the deletion of the gene and not in the oil-treated mice or control mice samples. Ctrl, control; CTX, chemotherapy; Tam, tamoxifen. **B.** Chemotherapy protocol comparison. We compared the protocols using cytarabine and doxorubicin described by Zuber *et al* (Zuber et al., 2009) and Wunderlich *et al* (Wunderlich et al., 2013). The Wunderlich *et al* protocol was developed for human AML xenografts in chemotherapy-sensitive NSG mice. It showed little effect on our murine AML model, so we decided to use the one described by Zuber *et al,* with a significant effect on blood parameters. Data shown from 1 experiment (n=4 mice/group). **C.** Cell-dose titration. Latency of the disease was analysed with two different clones (SM62 and SM63) and 3 different cell-doses ($10^3$, $10^4$ and $10^5$ cells) to adjust the timing of the protocol to the latency of the disease. Data shown from 1 experiment (n=3-4 mice/group). We finally chose to inject $10^4$ cells/mouse due to the more homogeneous results: all mice developed the disease and the latency was long enough to administer the two drug regimens. ip, intraperitoneal injection, iv: intravenous injection; WBC, white blood cells; RBC, red blood cells.

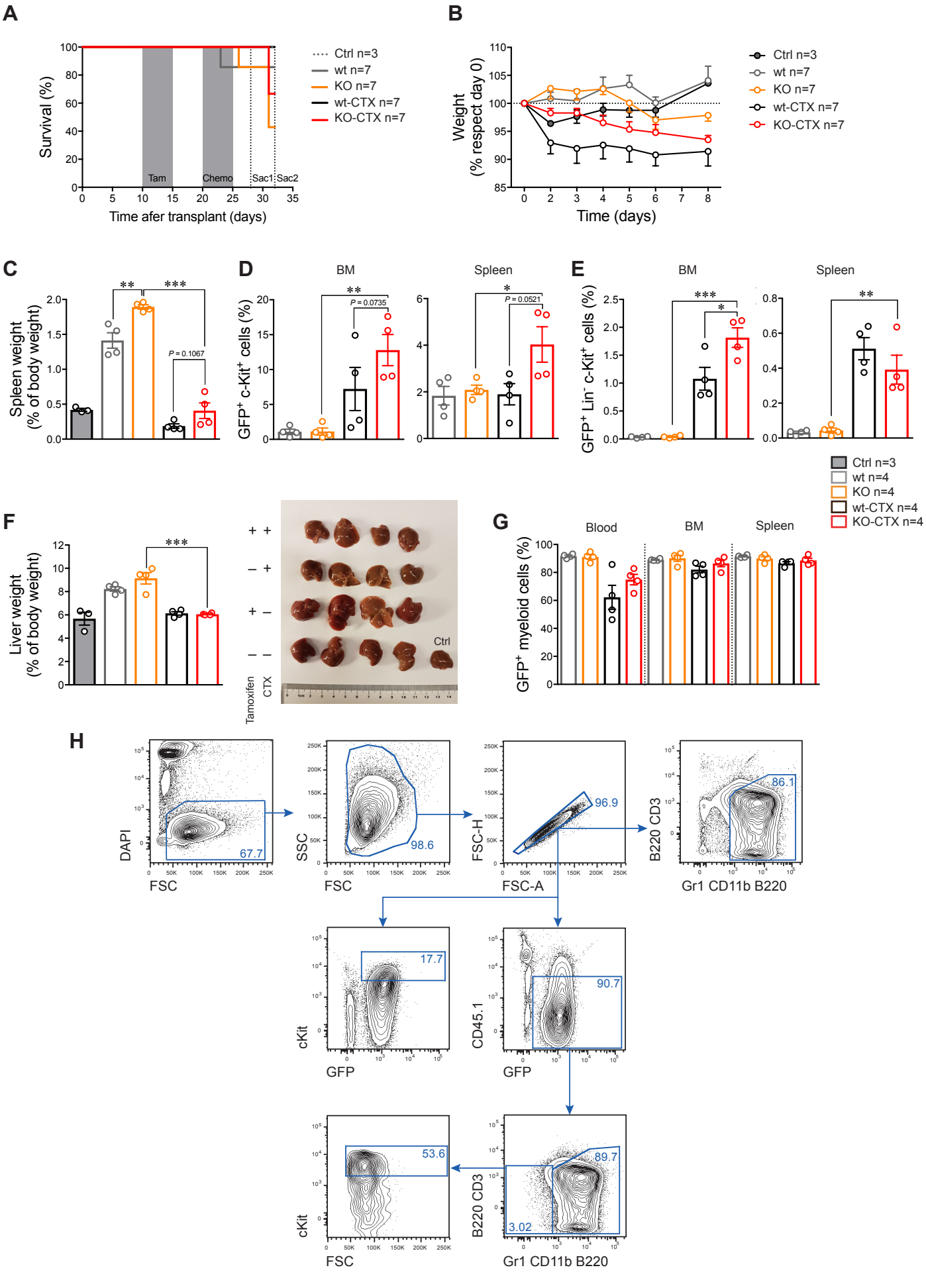
A
Survival (%)
Time afer transplant (days)
Tam
Chemo
Sac1
Sac2
Ctrl n=3
wt n=7
KO n=7
wt-CTX n=7
KO-CTX n=7
B
Weight (% respect day 0)
Time (days)
Ctrl n=3
wt n=7
KO n=7
wt-CTX n=7
KO-CTX n=7
C
Spleen weight (% of body weight)
P = 0.1067
D
BM
Spleen
GFP+ c-Kit+ cells (%)
P = 0.0735
P = 0.0521
E
BM
Spleen
GFP+ Lin- c-Kit+ cells (%)
Ctrl n=3
wt n=4
KO n=4
wt-CTX n=4
KO-CTX n=4
F
Liver weight (% of body weight)
Tamoxifen
CTX
Ctrl
G
Blood
BM
Spleen
GFP+ myeloid cells (%)
H
DAPI
FSC
67.7
SSC
98.6
FSC-H
FSC-A
96.9
B220 CD3
Gr1 CD11b B220
86.1
cKit
GFP
17.7
CD45.1
90.7
53.6
89.7
3.02

**Supplemental Figure 2, related to Figure 1.**

**A.** Survival curve of the analysed mice along the timeline of the experiment. **B.** Weight of the mice after chemotherapy treatment (first injection at day 1) showing the expected effect of loss of weight in the chemotherapy-treated animals. **C.** Spleen weight of the analysed animals at day 28 after transplantation showing a significant increment in liver size in the PBS-treated animals. **D-E.** Percentage of the $GFP^+$ $c\text{-}Kit^+$ (**D**) and $GFP^+$ $Lin^-$ $c\text{-}Kit^+$ (**E**) populations in BM and spleen of the analysed mice at day 28 after transplantation. **F.** Liver weight of the analysed animals at day 28 after transplantation showing a significant increment in liver size in the PBS-treated animals. **G.** $GFP^+$ myeloid cells in different organs in the analysed mice at day 28 after transplantation indicating a overtaking expansion of the injected cells in the myeloid compartment. Plots represent mean ± SEM. * $P < 0.05$, ** $P < 0.01$, *** $P < 0.01$. CTX, chemotherapy; Ctrl, control; sac, sacrifice; BM, bone marrow. **H.** Gating strategy used to analyse the different studied populations by flow cytometry. For the identification of the desired populations, dead cells were discarded by DAPI staining, intact cells were identified by FSC/SSC, duplets removed by FSC-A/FSC-H, myeloid cells were identified by Gr1 and CD11b staining, donor cells were identified by being negative for CD45.1 and positive for GFP and lineage negative cells were considered as those negative for CD3, B220, Gr1 and CD11b. FSC, forward scatter; SSC, side scatter; FSC-A, forward scatter-area; FSC-H, forward scatter-height.

Supplemental Figure S3. Velasco-Hernandez et al

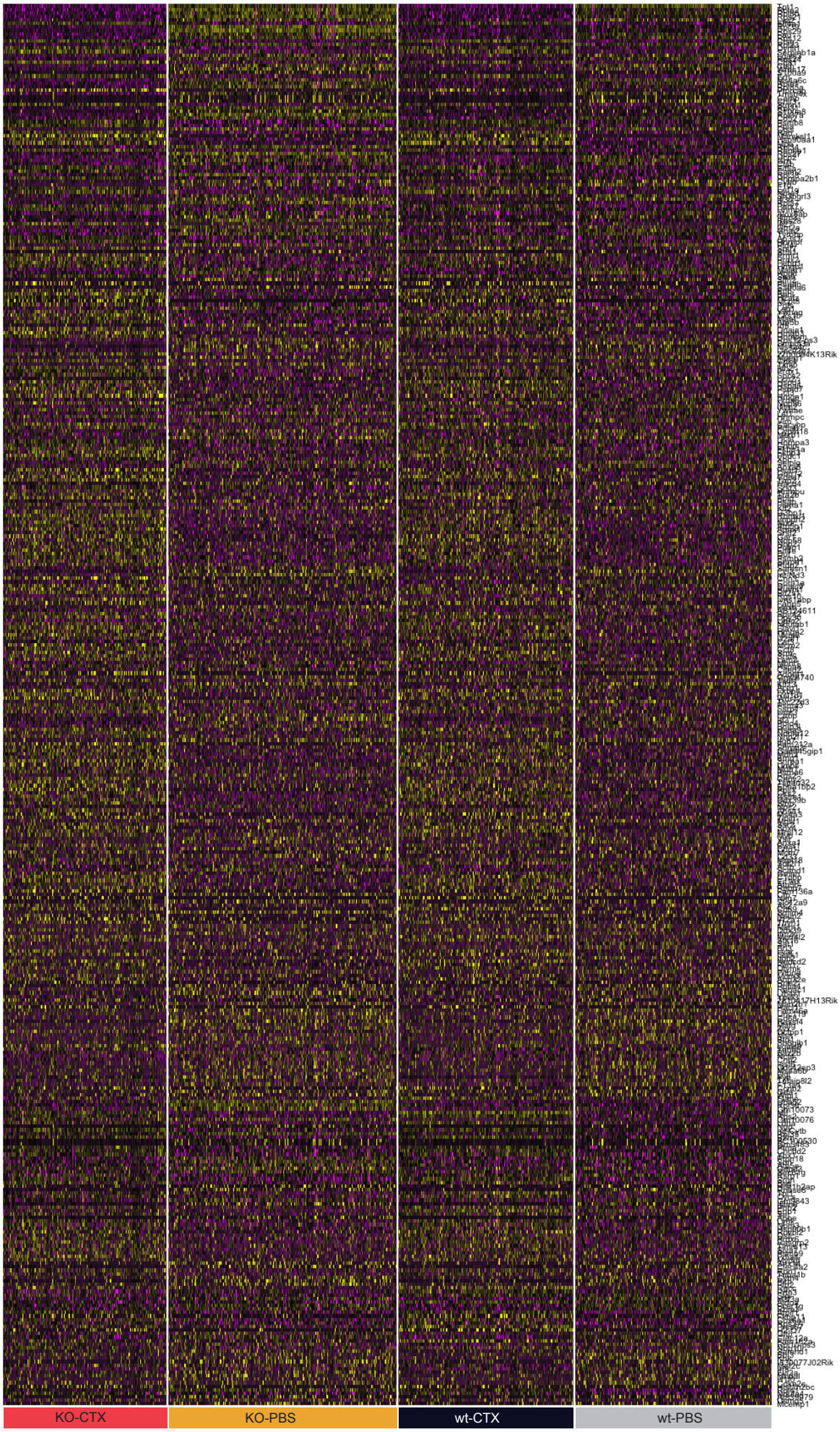

**Supplemental Figure 3, related to Figure 3.**

Heatmap depicting the 331 genes identified as differentially expressed among groups.

Supplemental Figure S4. Velasco-Hernandez et al

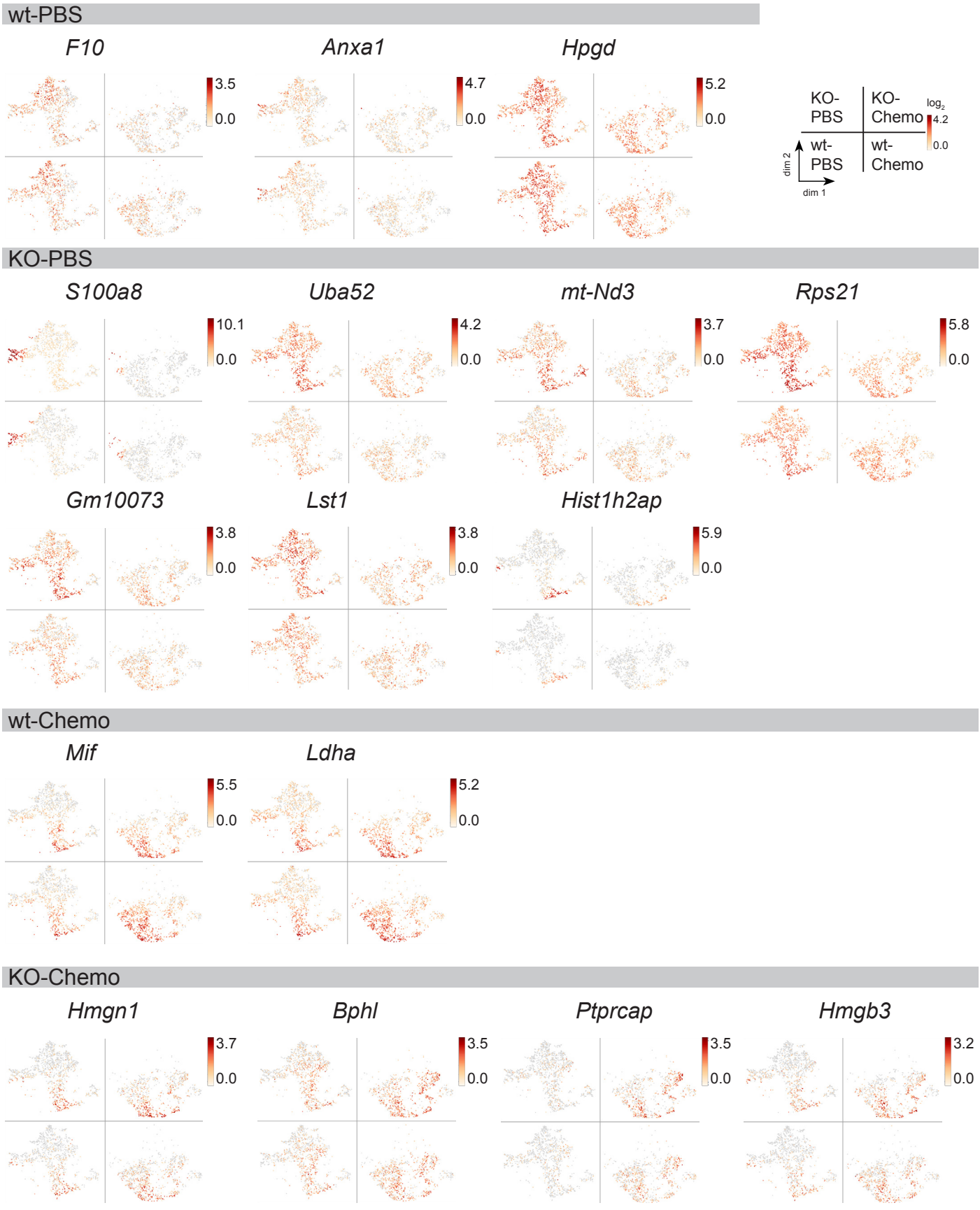

**Supplemental Figure 4, related to Figure 3.**

t-SNE plots showing the expression of uniquely differentialy expressed genes from each group in each individual cell. The scale at the right of each plot indicates the fold change expression ($log_2$).

## Supplemental Experimental Procedures:

### Mice

*Hif-1α*$^{lox}$ mice (Ryan et al., 2000) (JAX 007561) were crossed with the tamoxifen-inducible Rosa26Cre-ER$^{T2}$ mice (Ventura et al., 2007) (JAX 008463) to generate a combined conditional knock out (KO) model. Mice were maintained at the animal facility of the Biomedical Center at Lund University (Sweden) and all experiments were performed with consent from a local ethics committee.

### Retroviral transduction

A MLL-AF9 (MigR1-MLL-AF9-GFP) retroviral vector was used for retrovirus production. Retroviral supernatants were obtained by transient transfection of amphotropic Phoenix cells and supernatants were harvested after 48 h (Velasco-Hernandez et al., 2014).

BM from 8-12-week-old mice was harvested from pooled femora, tibiae and ilia by crushing in phosphate buffer saline (PBS) (Gibco) + 2% fetal calf serum (FCS) (Gibco) using a mortar and pestle. c-Kit+ cells were isolated using a magnetic separation system (MACS) and anti-c-kit magnetic beads (Miltenyi Biotec). Cells were cultured in StemSpan™ serum-free expansion media (Stem Cell Technologies) supplemented with 100 U/mL Penicillin/Streptomycin (Gibco), 20 ng/mL mIL3, 50 ng/ml hIL6, 50 ng/ml hTPO and 50 ng/mL mSCF (all from Peprotech) for 24 h. Transductions were performed by centrifugation of the retrovirus (2 h, 1000 g, 32°C) over retronectin- (Takara) coated plates (according to manufacturer's instructions) and co-culture of the c-Kit$^{+}$ cells over

the virus-coated wells for 24 h at 37°C. We used an MOI of 0.2, resulting in a transduction efficiency of 2% after 48 h. Cells were transplanted 24 h after transduction.

**Transplantations, drug administration and monitoring of mice**

Eight- to 12-week-old B6SJL x C57BL/6J (CD45.1-CD45.2) recipient mice were lethally irradiated with 900 cGy 4 to 15 h prior to transplantation. 5 x $10^5$ cells were intravenously (i.v.) injected into the tail vein of recipient mice together with 1 x $10^5$ freshly isolated total BM support cells from B6SJL (CD45.1) mice.

For secondary transplants, $10^4$ $GFP^+$ cells were i.v. injected into sublethally irradiated (500 cGy) recipient mice without support cells. Mice were kept on antibiotics (Ciproxin, Accord) in drinking water for 14 days after transplantation. Clonal leukemic cells were harvested 16 weeks after transplantation when mice started displaying signs of disease.

In secondary recipients, *Hif-1α* deletion was induced at day 10 after transplantation by intraperitoneal injection (i.p.) of 100 µL tamoxifen (10 mg/mL) (Sigma) on 4 consecutive days. As control, the same volume of the vehicle (peanut oil, Sigma) was injected into separate mice. *Hif-1α* deletion was verified by polymerase chain reaction (PCR) analysis of BM cells using the following primers: HIF-24: 5' –GCAGTTAAGAGCACTAGTTG-3', HIF-26: 5' –TTGGGGATGAAAACATCTGC-3'.

Chemotherapy treatment was performed as described by Zuber *et al* (Zuber et al., 2009): i.p. injection of 100 mg/kg cytarabine (Hospira) on 5 consecutive days and 3 mg/kg doxorubicin (Actavis) for 3 days. We started the treatment at day 20 after transplantation.

Three and 5 days after completion of the chemotherapy treatment, samples were collected from PB, BM, spleen and liver. Total white blood cell (WBC) counts were determined by an automated cell counter (KX-21N, Sysmex).

**Fluorescence-activated cell sorting analysis**

Expansion of leukemic cells was analysed by flow cytometry analysis of PB, BM and spleen cells. PB was lysed with ammonium chloride (Stem Cell Technologies) before staining. 4,6 diamino-2-phenylindole (DAPI) (Sigma) was used to exclude dead cells. The following antibodies were used to determine expansion of the leukemic cells: Gr-1-PE (RB6-8C5), CD11b-PE (M1/70), B220-PE/APC (RA3-6B2), CD3-APC (145-2C11), CD45.1-PECy7 (A20) (BioLegend) and c-Kit-APC-eFluor780 (2B8) (eBioscience). Samples were analysed using a LSRII cell analyser (BD Bioscience) and data analysed with FlowJo software (TreeStar).

**Limiting-Dilution Analysis**

***In vitro***

4, 8 or 12 $GFP^+$ BM cells were sorted into 96 wells of two U-bottom 96-well plates *per* sample with 100 μL of OptiMEM (Sigma) with 10% FCS (Gibco), 100 μM β-mercaptoetanol (Gibco), 50 μg/mL Gentamicin (Gibco), 10 ng/mL mSCF, 5 ng/mL mIL3 and 5 ng/mL G-CSF (all from PeproTech). Live ($DAPI^-$) and $GFP^+$ cells were sorted using a FACSAriaII cell sorter (BD Bioscience). One plate from each sample was incubated under normoxic conditions (20% $O_2$, 5% $CO_2$, 37°C) and other under hypoxic conditions (1% $O_2$, 5% $CO_2$, 37°C) for 10 days. Positive wells were scored when a visible colony was present.

***In vivo***

Eight- to 12-week-old CD45.1 or CD45.1-CD45.2 recipient mice were sublethally irradiated with 500 cGy 4 to 15 h prior to transplantation. 10, $10^2$, $10^3$ or $10^4$ $GFP^+$ BM cells were injected into the tail vein of recipient mice (n=4-6/group).

**Single-cell RNA-sequencing**

$GFP^+$ BM cells were sorted, washed and resuspended into PBS (Gibco) containing 0.04% ultrapure bovine serum albumin (BSA) (Ambion). Four biological replicates per sample were pooled after sorting. Cellular suspensions (target recovery of 1500 cells), Gel Beads and Partitioning Oil were loaded onto the Chromium A Chip (Chromium™ Single Cell A Chip Kit, 10x Genomics), and further into the Chromium Single Cell Controller (10x Genomics) for generation of single-cell Gel Bead-in-EMulsions (GEMs). Reverse transcription (RT) of the mRNA contained in the GEMs and subsequently single cell libraries for 3' RNA-seq, were prepared using Chromium™ Single Cell 3' Library & Gel Bead kit v2 (10x Genomics) according to manufacturer's instructions. In short GEM-RT was performed in a C1000 Touch™ Thermal cycler with 96-Deep Well Reaction Module (Bio-Rad): 53°C for 45 min, 85°C for 5 min; hold at 4°C. After RT, GEMs were broken, and cDNA was cleaned up using DynaBeads® MyOne™ Silane Beads (Thermo Fisher Scientific) and SPRIselect Reagent Kit (Beckman Coulter). cDNA was amplified using the C1000 Touch™ Thermal cycler with 96-Deep Well Reaction Module: 98°C for 3 min; cycled 13x: 98°C for 15sec, 67°C for 20sec, and 72°C for 1 min; 72°C for 1 min; hold at 4°C. After SPRIselect purification, the cDNA was fragmented enzymatically and indexed sequencing libraries were constructed using the reagents in the Single Cell Library Kit and Chromium™ i7

Multiplex Kit (10x Genomics) following these steps: 1) Fragmentation, end repair and A-tailing; 2) Post-fragmentation double sided SPRI selection; 3) Adaptor ligation; 4) Post-ligation cleanup with SPRIselect; 5) Sample index PCR and double sided SPRIselect cleanup. Sample index PCR were performed in a C1000 Touch™ Thermal cycler with 96-Deep Well Reaction Module: 98°C for 45 sec; cycled 14x: 98°C for 20 sec, 54°C for 30 sec, and 72°C for 20 sec; 72°C for 1 min; hold at 4°C. Quality and size of cDNA before fragmentation and post sample index PCR was determined using a High Sensitivity (HS) DNA kit (Agilent Technologies) loaded on a 2100 Bioanalyzer (Agilent Technologies). A final quantification of the barcoded libraries was achieved using quantitative PCR (qPCR) (KAPA Library Quantification Kit for Illumina platforms, KAPA Biosystems), before sequencing using a Nextseq500 (Illumina) was performed. Sequencing ready libraries were denaturated and diluted to 1.8pM according to Illumina instructions before loaded on Illumina NextSeq500 using a 150 cycles High output v2 kit (Illumina). Paired-end sequencing was performed with the following read lengths: Read1; 26 cycles, Read2; 98 cycles and 8 cycles of I7 Index. Two consecutive sequencing runs were performed to achieve enough sequencing depth and the data was combined. Reads were processed and UMIs counted using Cell Ranger v1.3.0 against the mm10 annotation. Downstream analyses were performed using Seurat v2.1.0 for R where the cells were filtered to remove potential doublets and scaled regressing out the effects of mitochondrial content and the number of UMIs attained from each cell. Differentially expressed genes were identified, and the cells were projected on two dimensions using TSNE.

**Differential expression analysis and pathway enrichment**

t-SNE plots and K-clustering were generated with Loupe software (10X Genomics).

Venn diagrams were generated with BioVenn (www.biovenn.nl) (Hulsen et al., 2008). Gene Functional Classification was performed using DAVID (david.ncifcrf.gov/home.jsp) (Huang da et al., 2009). Functional protein associations, GO and KEGG enrichment analysis were investigated using STRING (string-db.org) (Szklarczyk et al., 2015) and for the visualization of the networks we used Cytoscape (Shannon et al., 2003). A minimum interaction score of 0.5 was used to detect interactions.

**Statistical analysis**

All data are expressed as the mean ± SEM. Differences between groups were assessed using unpaired Student's *t* tests. All analyses were performed with Prism software, version 7.0 (GraphPad software). Frequency estimations were generated using Extreme Limiting Dilution Analysis (ELDA) software, which takes into account whether the assumptions for LDA are met (http://bioinf.wehi.edu.au/software/elda/) (Hu and Smyth, 2009).

## Supplemental References

Hu, Y., and Smyth, G.K. (2009). ELDA: extreme limiting dilution analysis for comparing depleted and enriched populations in stem cell and other assays. Journal of immunological methods *347*, 70-78.

Huang da, W., Sherman, B.T., and Lempicki, R.A. (2009). Systematic and integrative analysis of large gene lists using DAVID bioinformatics resources. Nature protocols *4*, 44-57.

Hulsen, T., de Vlieg, J., and Alkema, W. (2008). BioVenn - a web application for the comparison and visualization of biological lists using area-proportional Venn diagrams. BMC genomics *9*, 488.

Shannon, P., Markiel, A., Ozier, O., Baliga, N.S., Wang, J.T., Ramage, D., Amin, N., Schwikowski, B., and Ideker, T. (2003). Cytoscape: a software environment for integrated models of biomolecular interaction networks. Genome research *13*, 2498-2504.

Szklarczyk, D., Franceschini, A., Wyder, S., Forslund, K., Heller, D., Huerta-Cepas, J., Simonovic, M., Roth, A., Santos, A., Tsafou, K.P.*, et al.* (2015). STRING v10: protein-protein interaction networks, integrated over the tree of life. Nucleic acids research *43*, D447-452.